EXPERIMENTAL INVESTIGATION AND MODELLING OF FLOW AND TURBULENCE IN A SWIRL COMBUSTOR

R. Palm, S. Grundmann, S. Jakirlić and C. Tropea
Chair of Fluid Mechanics and Aerodynamics,
Darmstadt University of Technology
Petersenstr. 30, D-64287 Darmstadt, Germany
s.jakirlic@sla.tu-darmstadt.de

1. ABSTRACT

The interaction between a swirling annular jet and a central, non-swirling stream expanding into a model of a tuboannular combustor was investigated experimentally using Particle Image Velocimetry (PIV) under conditions of variable swirl intensity ($0.0 < S < 1.2$) and mass flow rate ratio. Two flow domains in the $x-r$ plane were measured covering the most intense regions of mixing immediately after the sudden expansion. The focus of the investigation was on the swirl intensity influence on the size and shape of the backflow region being generated in the flow core. In addition, the numerical computations of the entire experimental configuration including swirl generator, inlet section and the combustor (flue) itself using a version of the Second-Moment Closure (SMC) model were performed. The results obtained demonstrate gradual expansion of the free recirculation zone into the radial direction with the separation onset shifted upstream towards the combustor entrance under increasing swirl intensity.

2. INTRODUCTION

The mixing of the swirling annular jet (primary air) and the non-swirling inner jet (fuel) represents one of the most important processes in a gas turbine swirl combustor, influencing to a large extent the efficiency of the entire combustion process. A recirculation zone generated in the center of a swirl combustor enhances flame stability and is a usual design concept of combustors. Additionally, the flow field is influenced by the effects of combustion in several ways. Even restricting the attention only to the isothermal case, an exceedingly complex flow pattern arises, exhibiting several simultaneously occurring phenomena. Numerous experimental investigations serving for years as benchmarks for computational methods and turbulence model validation have been conducted in the past. Roback and Johnson (1983) investigated flow and passive scalar transport in a single tubular model combustor with a swirling annular jet ($S = 0.41$) discharging into sudden expansion (expansion ratio 2.1). So et al. (1984) explored the combustor of similar type but with no expansion of the strongly swirling inflow ($S = 2.24$) and with a high-velocity central jet preventing the generation of a free recirculation zone. Dellenback[1] et al. (1988) and Nejad et al. (1989) investigated a pure swirling flow through an abrupt axisymmetric expansion covering the swirl intensity range up to $S = 0.5$.

The influence of the variable swirl intensity was among others also the topic of the present study. However, unlike previous work, the combustor model exhibited dimensions and operating conditions close to those encountered in a real combustor. To systematically study this flow configuration an experimental facility has been built which allows independent flow rate adjustment of the central (main stream) and co-axial (annular) jet flow ($\dot{V}_c/\dot{V}_m$). The measurements were performed over a range of swirl intensities and Reynolds numbers related to the main stream and swirling annular flow. The experimental facility also allows the investigation of the influence of the flow confinement in terms of variable expansion ratio ER (not covered here). This complex flow geometry is a good example of complementary experimental and numerical investigations. The experimental results can be used to verify turbulence models and numerical simulations, which can be used for parametric studies. One of the important goals was not only to study the flow and mixing under conditions encountered in a real combustor (high Reynolds and swirl numbers) but also to generate an extensive database which can be used for turbulence model validation. Prior to considering the flow within the flue, an intensive study of the flow structure entering the combustor was conducted. It was of decisive importance, keeping in mind that no data prior to the flow expansion is available in previous experimental investigations, Palm et al. (2005).

[1] Dellenback et al. (1994) investigated also a combustor model with a swirling inner jet and a non-swirling, non-expanding, annular stream with varying swirl intensity up to $S = 1.3$.

3. EXPERIMENTAL FACILITY

The operating parameters of the experimental facility (Fig. 1) are summarized in Table 1. These parameters have been chosen to represent values typical of a real combustor. The inner diameter of the main flow D_m is *36mm*. The inner diameter of the annular section is *40mm* and the outer diameter D_c is 100mm. The diameter of the flue D_f is 200mm.

Table 1: Operating flow conditions

Parameter	Range
Reynolds number (Main flow)	$23500 \le \mathrm{Re}_m \le 102000$
Mass flow rate; *kg/s* (Main flow)	$0.01 \le \dot{m}_m \le 0.05$
Reynolds number (Annular flow)	$49530 \le \mathrm{Re}_c \le 125500$
Mass flow rate; *kg/s* (Annular flow)	$0.1 \le \dot{m}_c \le 0.25$
Swirl intensities, *S*	$0 \le S \le 1.2$
Expansion ratio, *ER*	2

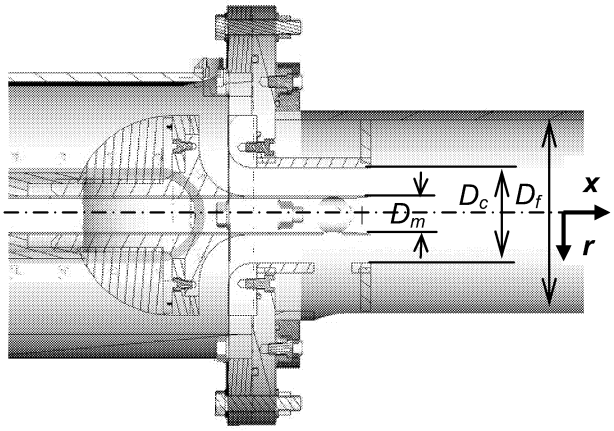

Figure 1: Combustion chamber model

The swirl generator is based on the "movable block" design, Leuckel (1969). By rotating an inner and an outer annular block relative to each other, varying degrees of tangential and radial channels will be created. With a pure radial inlet, a non-swirling flow is obtained, and with a pure tangential inlet, the maximum swirl is generated.

For measuring the velocity field, a PIV system was used. This measurement technique is characterized by a high spatial resolution. For statistical convergence, 1200 images were sufficient to generate a stable velocity vector map. A Solo PIV Nd: YAG Laser System from New Wave Research is used as a light source (λ=*532nm*). The output energy of the laser is 50mJ at a frequency of 15Hz. The images are acquired using a 12 Bit SensiCam from PCO. The signal and data processing has been carried out with the processor and software "Flow Manager" from Dantec-Dynamics. For data processing the adaptive correlation was used. It was necessary to dewarp and resample the images because of a small out-of-plane acquisition. Incense was used as tracer particles, having an estimated diameter of *1* μm, small enough to follow all expected flow fluctuations without noticeable slip.

4. RESULTS AND DISCUSSION

To give a first impression about the flow structure in a model combustor, a sketch of the mean flow pattern is shown in Fig. 2. The annular flow is swirled, inducing a strong recirculation in the core flow used for flame stabilization in combustors. The size, shape and position of this flow reversal zone depend strongly on the swirl intensity imposed and the volume rate ratio. The flow is further characterized by an annular, wall-bounded separation region, whose length is also influenced to a large extent by the swirled annular stream. The resultant shear/mixing layers are characterized by very high turbulence levels due to strong velocity gradients and strong streamline curvature, both conducive to good mixing prior to combustion, e.g. of a liquid fuel spray. While the statistical mean flow pattern is found to be axial-symmetric, the instantaneous flow fields, exhibiting a large range of vortices captured by the time-resolved PIV, are highly asymmetric. However, statistical mean fields are suitable for comparison with simulations within the RANS framework. Experimentally two flow domains in the $x-r$ plane were measured, shown as dashed areas in Fig. 2. These regions (up to $x/D_f = 1$) were suspected to cover the most intense regions of mixing.

Some selected experimental results are displayed in the following figures. They are selectively compared with the computational results, obtained by a two-layer version of the basic high-Reynolds number Second-Moment closure model proposed by Gibson and Launder (1978) with variable model coefficients due to Launder and Shima (1989). In the near-wall layer a one-equation model based on the transport equation for the kinetic energy of turbulence was solved. The flow domain adopted covers the entire inlet section including swirl generator system with both central and annular pipes and the flue itself. Such an approach provides well-defined initial conditions. 3-D computations of the swirl generator system (only one eighth of the configuration, meshed by ca. 150000 cells, was accounted for) and 2-D (axysymmetric) computations of the part of the inlet section and the flue (see e.g., Fig. 5, meshed by ca. 25000 cells providing the dimensionless

wall distance of the wall-closest cell was $y^+ < 1$) were performed separately using commercial CFD-software (FLUENT). The profiles of all variables across the inlet section (annular and central pipe) for the flue computation were prescribed from the data obtained computing the 3-D swirl generator system (Palm et al., 2005). The computations performed represent preliminary numerical work aimed primarily at identifying important features that require special consideration in turbulence modelling. More detailed modelling efforts are planned for the future.

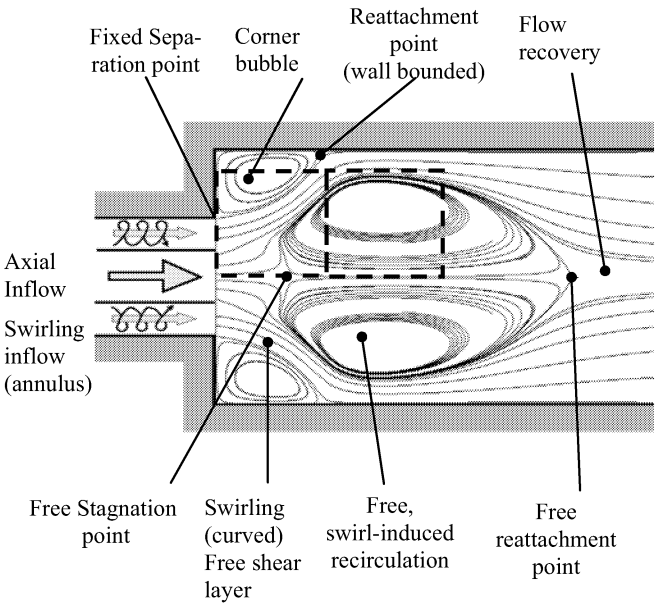

Figure 2: Schematic of air flow in an idealized combustion chamber

4.1 Swirl intensity influence

Figs. 3 to 10 show the influence of the swirl intensity on the mean flow structure illustrated by the time-averaged streamlines (Figs. 3-5), iso-contours of the mean axial and radial velocity fields (Figs. 6-7) and axial velocity and turbulent quantity profiles at selected locations (Figs. 8-10) in the near field of the flow within the flue by keeping constant the ratio of the outer (annular stream at $\mathrm{Re}_c = 125500$) flow rate $\dot{V}_c$ to the inner (mean stream at $\mathrm{Re}_m = 47000$) one $\dot{V}_m$: $\dot{V}_c / \dot{V}_m = 10$. The corresponding Reynolds number of the flow inside the flue was $\mathrm{Re}_f = 96000$. All represented quantities are normalized by the bulk velocity of the flow within the flue, U_f. It should be noted that only the flow domain up to $x/D_f = 0.94$ and $y/D_f = 0.4$ was mapped by PIV. Also, the circumferential velocity field could not be captured by the PIV system applied. The non-swirling flow configuration (Fig. 3) is characterized by a long annular (wall-mounted) corner bubble. Besides a corner bubble (which is of substantially shorter length compared to the non-swirling case), the most important feature of the swirling flow configuration is a large (swirl-induced) free separation region in the core flow, Figs. 4 and 5.

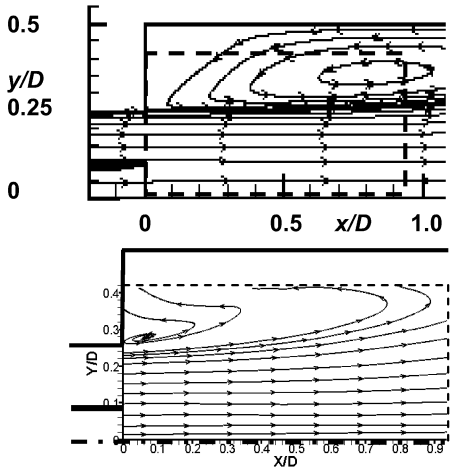

Figure 3: Computationally (upper) and experimentally (lower) obtained streamlines (*S=0*, U_c/U_f=*4.4*, U_m/U_f=*2.7*)

A short wake region between the inner and annular streams passes into a large-eddy shear region between both recirculation zones. The most intensive turbulence production, and finally mixing, occurs just in this flow region bordering both the central and corner bubbles.

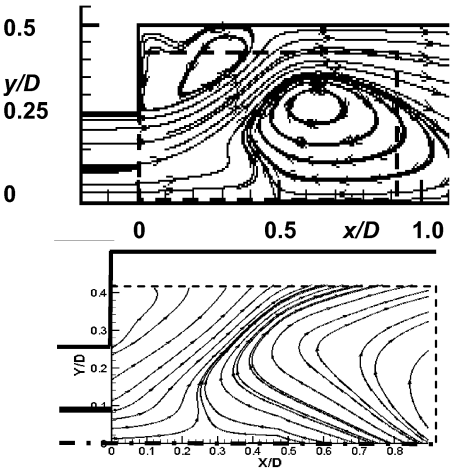

Figure 4: Computationally (upper) and experimentally (lower) obtained streamlines (*S=0.6*, U_c/U_f=*4.4*, U_m/U_f=*2.7*)

In addition to the large mean velocity gradients due to the sudden expansion, the process of turbulence generation is further influenced by an extra strain rate originating from the streamline curvature. Figs. 4-7 illustrate the intensification of the velocity magnitude (with respect to both the

shear layer and the backflow region) and the strengthening of the curvature of the shear layer by increasing the swirl intensity. The radial flow becomes more intensive, hence promoting the mixing. Whereas the annular swirling jet separates at the sharp edge of the sudden expansion, generating the corner bubble, both the separation and reattachment points of the large recirculation zone are situated on the combustor centerline i.e. in the free stream.

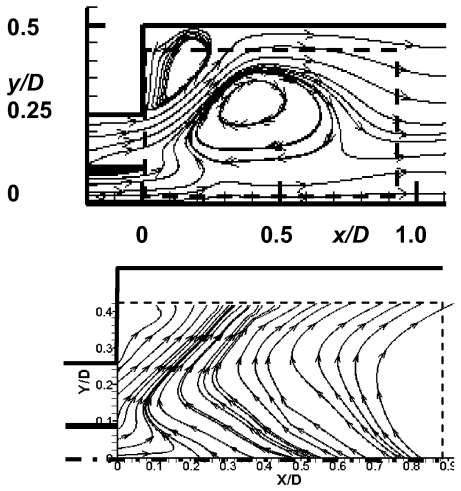

Figure 5: Computationally (upper) and experimentally (lower) obtained streamlines (*S=1.2*, U_c/U_f*=4.4*, U_m/U_f*=2.7*)

This swirl-induced separation represents actually a transition from the supercritical flow state related to the non-swirling central stream to the sub-critical situation with respect to the flow reversal in the core (vortex breakdown phenomena; Escudier and Keller, 1985). The flow situation presented here corresponds to the locally sub-critical state in accordance to the flow recovery after passing through the central backflow region. It contributes significantly to the corner bubble shortening, Figs. 3 to 5. The increasingly curved, swirling shear layer and the position of the free separation and reattachment points are of great importance for characterisation of the free recirculation with respect to the mixing within the combustor. The basic mechanism behind the mixing intensification is the retardation of the axial momentum immediately after sudden expansion, manifested through its transformation into the radial and angular momentum having the highest intensity in the interface region between the corner and free bubbles. The final outcome is the propagation of the free separation point towards the flue entrance with increasing swirl intensity. In the case with moderate swirl intensity ($S = 0.6$), the separation onset, that is the free-stagnation point, is established at the position $x/D_f \approx 0.3$. The free separation point is clearly shifted upstream towards the flue entrance to the position $x/D_f \approx 0.2$ for the case with the highest swirl $x/D_f \approx 0.2$ for the case with the highest swirl intensity $S = 1.2$. It could also be deduced from the Figs. 9 and 10 displaying axial velocity profiles.

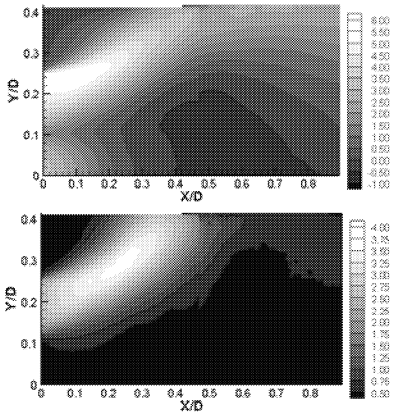

Figure 6: Experimental results (*S=0.6*, U_c/U_f*=4.4*, U_m/U_f*=2.7*), U/U_f (upper figure), V/U_f (lower figure)

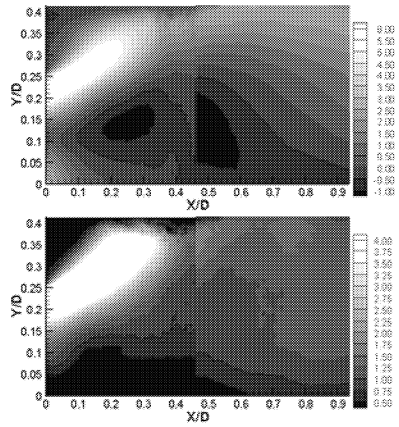

Figure 7: Experimental results (*S=1.2*, U_c/U_f*=4.4*, U_m/U_f=2.7), U/U_f (upper figure), V/U_f (lower figure)

Proper prediction of the separation onset and reattaching length of such a free bubble represents a special challenge for statistical turbulence models. The computational results for the non-swirling and moderately swirling ($S = 0.6$) cases (Figs. 3, 4 and 8) shows a good qualitative agreement with the experimental results. However, the flow separates substantially later, approximately at x/D_f*=0.5*, Figs. 4 and 8. The mean dividing streamline penetrates towards combustor inlet up to the location ($x/D_f \approx 0.35$; $y/D_f \approx 0.15$) corresponding to the radial position of the shear layer generated between central and annular streams. This position is characterized by the maximum negative value of the axial velocity. The size of this free separation zone with respect to its diameter agrees well with the experimental result. The information about its length, that is the position of the free reat-

tachment point, cannot be deduced from the available body of experimental data. The negative axial velocities at the position $x/D_f=0.8$ at combustor centerline, corresponding to the last measurement position, obtained by both experiment and computations agree well.

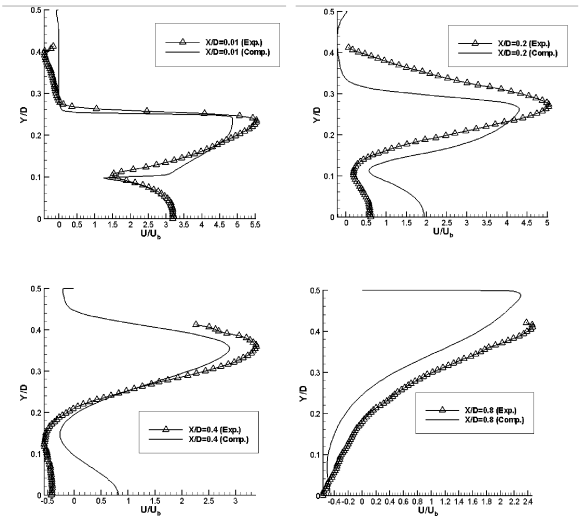

Figure 8: U/U_f ($S=0.6$, $U_c/U_f=4.4$, $U_m/U_f=2.7$), ($x/D=0.01$, $x/D=0.2$, $x/D=0.4$ and $x/D=0.8$)

The comparison of the experimental and computational results obtained for the highest swirl intensity $S=1.2$ reveals very interesting mean flow features, Figs. 5, 7 and 9. Whereas the experimental data show clearly the existence of the large (larger than in the previous case) central recirculation zone starting at $x/D_f\approx0.2$ and ending far outside of the experimentally covered flow region, the computations result in a separation region, whose onset is not situated at the symmetry axes, Fig. 5 upper. The computationally obtained separation zone is lifted in the radial direction exhibiting an annular form, with a central jet going through the middle (note the continuously positive value of the centerline velocity, Fig. 9). The origin of such anomaly could lay in the poor representation of the swirling flow in the annular pipe (note the separation of the flow at the inner wall, Fig. 5 upper and Fig. 9, position $x/D_f=0.01$). Such a strong angular momentum propagates in the radial direction weakening the influence of the swirl on the axial motion in the core flow. A similar outcome was obtained experimentally for the higher velocities of the central jet relative to the velocity of the annular jet (lower volume flow ratio, see Fig. 11). The exact length of the free separation zone for the highest swirl intensity was not experimentally captured. By comparing the axial velocity profiles at the last measurement position $x/D_f=0.8$ for the swirl intensities $S=0.6$ (Fig. 8) and $S=1.2$ (Fig. 9), the latter case exhibiting much higher negative velocity at the flue centerline, it is obvious that this zone is substantially larger.

Fig. 10 displays profiles of the streamwise and shear Reynolds stress components at two streamwise position, immediately after the sudden expansion $x/D_f=0.01$ and at $x/D_f=0.8$ for the highest swirl intensity case.

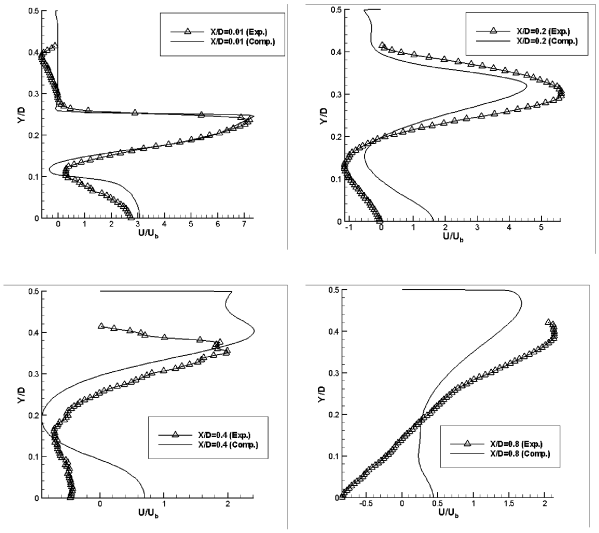

Figure 9: U/U_f ($S=1.2$, $U_c/U_f=4.4$, $U_m/U_f=2.7$), ($x/D=0.01$, $x/D=0.2$, $x/D=0.4$ and $x/D=0.8$)

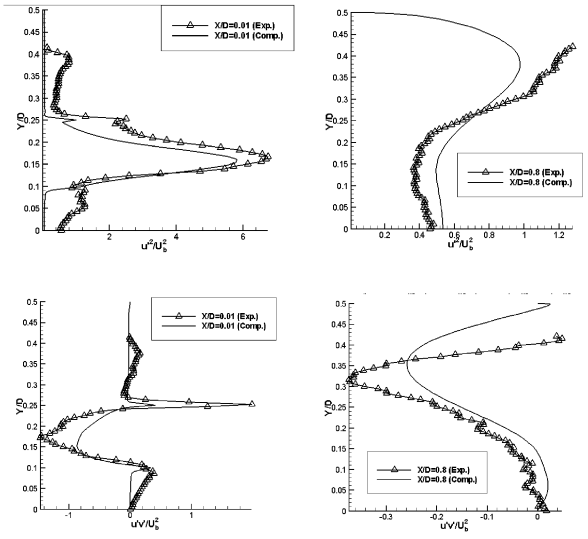

Figure 10: $\overline{u^2}/U_f^2$ (upper) and $\overline{uv}/U_f^2$ (lower) at two streamline locations in the fuel ($S=1.2$, $U_c/U_f=4.4$, $U_m/U_f=2.7$), ($x/D=0.01$, $x/D=0.2$, $x/D=0.4$ and $x/D=0.8$)

As expected, the highest turbulence level is captured within the shear layer regions. The figures document also a high level of the turbulence decay at the presented combustor length. The initial level of turbulence ($x/D_f=0.01$) obtained computationally by accounting for the complete

inlet system including swirl generator is lower compared to experimentally obtained values. This is especially the case in the central portion of the flow. Further analysis is in progress.

4.2 Volume ratio influence

The influence of the volume rate ratio $\dot{V}_c/\dot{V}_m$ on the position, size and shape of the free recirculation zone by keeping constant the swirl intensity ($S=1.2$) is illustrated in this section. The volume rate ratio is changed by increasing/decreasing the volume rate of the inner (non-swirling) jet, while the volume rate of the annular (swirling) jet was kept constant. This is the same volume rate $\dot{V}_c$ (corresponding to $\mathrm{Re}_c=125500$), analyzed in the previous section. Two additional volume rate ratios considered are $\dot{V}_c/\dot{V}_m=5$ (corresponding to $\mathrm{Re}_m=102000$ and $\mathrm{Re}_f=106550$), Fig. 11 and $\dot{V}_c/\dot{V}_m=25$ (corresponding to $\mathrm{Re}_m=23500$ and $\mathrm{Re}_f=91325$), Fig. 12.

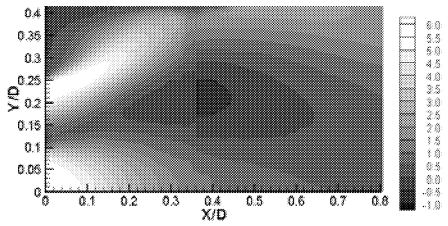

Figure 11: Experimental result, U/U_f ($S=1.2$, $U_c/U_f=3.9$, $U_m/U_f=5.3$)

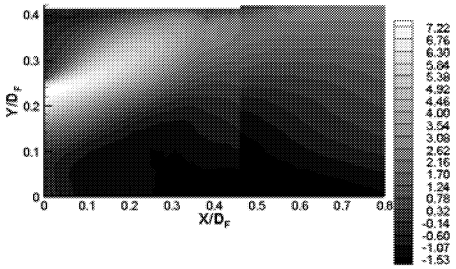

Figure 12: Experimental result, U/U_f ($S=1.2$, $U_c/U_f=4.6$, $U_m/U_f=1.4$)

These figures, together with Fig. 7 ($\dot{V}_c/\dot{V}_m=10$), show clearly the behaviour of the core flow by varying the inner volume flow rate. By lower volume rate ratio (Fig. 11), the flow situation with the continuously positive centerline velocity will be established. The free recirculation zone takes the form of a ring-shaped vortex. A higher volume ratio (approximately 6 according to our measurements for the $S=1.2$ case) guarantees a stable vortex breakdown with the separation point (at the centerline) penetrating towards the nozzle exit. For the highest volume rate ratio measured ($\dot{V}_c/\dot{V}_m=25$; Fig. 12) a large free recirculation zone is obtained with the separation point situated even in the interior of the central pipe.

5. CONCLUSIONS

The effects of the increasingly swirled annular jet on the flow in a model combustor and the variable volume rate ratio of the outer (swirling) stream to the inner (non-swirling) one with respect to the position, size and shape of the swirl-induced free recirculation zone in a model combustor model were experimentally investigated. In addition, complementary computations were performed. The increasing swirl intensity contributes significantly to the intensification of the back-flow activity in the combustor core with free separation point penetrating towards the combustor inlet, hence promoting the mixing. It is further found, that the volume rate ratio represents an important parameter when controlling the topology of the flow reversal within combustor.

ACKNOWLEDGEMENTS. The financial support of the German Ministry for Education and Science (BMBF) through the grant 03TRA2AC (R. Palm) is gratefully acknowledged.

REFERENCES

[1.] Dellenback, P.A., Metzger, D.E., and Neitzel, G.P. (1988): Measurements in turbulent swirling flow through an abrupt axisymmetric expansion. *AIAA J.*, Vol. **26(6)**, pp. 669-681

[2.] Dellenback, P.A., Sanger, J.L. and Metzger, D.E. (1994): Heat transfer in coaxial jet mixing with swirled inner jet. *ASME J. Heat Transfer*, Vol. **116**, pp. 864-870

[3.] Escudier, M.P., and Keller, J.J. (1985): Recirculation in Swirling Flow: A Manifestation of Vortex Breakdown. *AIAA J.*, Vol. **23**, No. **1**, pp. 111-116

[4.] Nejad, A.S., Vanka S.P., Favaloro, S.C, Samimy, M. and Langenfeld C. (1989*):* Application of Laser Velocimetry for Characterization of Confined Swirling Flow. *ASME J. Eng. For Gas Turbines and Power*, Vol. **111**, pp. 36-45

[5.] Palm, R., Grundmann, S., Weismüller, M., Šarić, S., Jakirlić, S. and Tropea, C. (2005): Experimental characterization and modelling of inflow conditions for a gas turbine swirl combustor. *6th Symposium on Engineering Turbulence Modelling and Measurements*, Sardinia, Italy, May 23-25

[6.] Roback, R., and Johnson B.V. (1983): Mass and Momentum Turbulent Transport Experiments with Confined Swirling Coaxial Jets. *NASA Contractor Report 168252*

[7.] So, R.M.C., Ahmed, S.A., and Mongia H.C. (1984): An Experimental Investigation of gas Jets in Confined Swirling Air Flow. *NASA CR 3832*